1

LEO Satellite Ground Station Design Concepts

1.1 An Overview of LEO Satellites

Satellites are an important part of telecommunication infrastructure worldwide, carrying large amounts of multimedia traffic. Since their inception around 60 years ago, communication satellites have been a major element in worldwide communication infrastructure and networking. More than 40 countries own satellites for communication, commercial, science, and even humanitarian purposes. But only few of them have building and launching capabilities.

The basic resources available for satellite communications are orbits and radio frequency (RF) spectrum. The orbit is the path in space followed by the satellite; the frequency allocations are subject to international agreements managed and controlled by international bodies.

Different types of orbits are possible, each suitable for a specific application or mission. Generally, satellites follow an elliptical orbit with a determined eccentricity laid on the orbital plane defined by space orbital parameters (Maral and Bousquet 2005; Maini and Agrawal 2011). Thus, the space orbital parameters, known as Kepler's elements (usually given as two-lines elements), determine the position of the satellite in space (space slot). Orbits with zero eccentricity are known as circular orbits. The circularity of the orbit simplifies the analysis, compared to the elliptical one. The movement of the satellite within its circular orbit is represented by altitude, radius velocity, and orbital time.

Satellites' circular orbits are categorized as geosynchronous Earth orbits (GEO), medium Earth orbits (MEO), and low Earth orbits (LEO). The main difference among them is in the altitude above the Earth's surface, which further impacts the velocity and the orbital period of the satellite in the appropriate orbit (Maral and Bousquet 2005; Maini and Agrawal 2011). Only the circular orbits are of the further concern through this book, more exactly, the LEO satellites and the appropriate ground stations.

Communication between the satellite and a ground station is established when the satellite is consolidated in its own orbit and it is visible from the ground station. The link that transmits radio waves from the ground station to the satellite is called uplink, and from satellite toward the ground station is downlink.

The orbits of altitudes ranging from 300 km up to around 1400 km above the Earth's surface are defined as LEO, and the satellites consolidated to these orbits are known as the LEO satellites. The lower altitude range is limited by the Earth's atmosphere – more accurately, by the level above the Earth's atmosphere where there is almost no air, so the satellite's speed reduction and drag down is avoided. The inner Van Allen belt limits the higher altitude range (Van Allen radiation belt 2020). The Van Allen belt is known as a space radiation zone and has undesired effects on satellites'

Ground Station Design and Analysis for LEO Satellites: Analytical, Experimental and Simulation Approach, First Edition. Shkelzen Cakaj.

payload and platform (electronic components and solar cells can be damaged by this radiation); thus, the belt should not be used for the accommodation of LEO satellites.

LEO satellites move at around 7.2–7.5 km/s velocity relative to a fixed point on the Earth (ground station). Satellites' orbital period is in the range of 90–110 minutes. The communication duration between the satellite and the ground station takes 5–15 minutes over 6–8 times during the day (Cakaj and Malaric 2007a), all these dependent on orbital altitude. The characteristics of LEOs are the shortest distance from the Earth compared with other orbits and consequently less time delay. These characteristics make them very attractive for communications but also for other applications (Cakaj 2021).

Thus, in addition to communications, LEO satellites are also applied for scientific and research purposes, more specifically under circumstances where no on-ground means are appropriate. Dynamics on climate changes, remote sensing applications for oceans, different astronomic observations, ions density records in the ionosphere, and very specific humanitarian applications related to search and rescue services are some of activities carried out by LEO satellites, activities that are too difficult or impossible to be implemented on Earth. For these activities within satellite structures, the instruments or devices (telescope, cameras, probes, sensors, etc.) for the appropriate application or mission are installed (Zee and Stibrany 2002; Cakaj et al. 2010a). Usually, LEO satellites dedicated for scientific purposes or remote sensing applications are accommodated in specifically designed orbits, known as the Sun synchronized orbit. The Sun synchronization feature enables a treated area on the ground from the satellite to be observed under similar illumination conditions due to different satellite passes (Cakaj et al. 2009).

These satellites provide opportunities for investigations for which alternative techniques are either difficult or impossible to apply. Thus, it may be expected that such missions will be further developed soon, especially in fields where similar experiments by purely Earth-based means are impracticable. Ground stations (access points) must be established to communicate with such satellites, and the quality of communication depends on the performance of the satellite ground station, in addition to that of the satellite.

Communications-integrated satellite-terrestrial networks used for global broadband services have gained a high degree of interest from scientists and industries worldwide. The most convenient structures for such use are LEO satellites, since they fly closer to the Earth compared to the other orbits, and consequently provide significantly lower latency, which is essential for reliable and safe communications. Among these efforts is the *Starlink* satellites constellation, developed and partly deployed by the US company SpaceX. The constellation is planned to be organized in three spatial shells, each made up of several hundreds of small-dimensioned and lightweight LEO satellites specially designed to provide broadband services, intending to offer global Earth coverage through their interoperability, combined with the ground stations as a part of the satellite-terrestrial integrated network. On October 24, 2020, 893 satellites were situated in orbit of altitudes of 550 km under different inclinations, determining the first *Starlink* orbital shell (Cakaj 2021).

This would suggest that in the near future, worldwide broadband services provided by integrated satellite-terrestrial communication networks will be a part of daily communication activities, demands for which will rapidly increase, so operators should carefully manage operation and distribution of real-time services toward maximizing the downlink data throughput related to the broadband requirements without significantly affecting the mission cost (Botta and Pescape 2013; Garner et al. 2009). Therefore, future satellite payloads and platforms must become more flexible, lightweight, and smaller, easier to be launched, and reconfigurable related to the EIRP and coverage, to provide large capacity at the lowest cost, toward the main goal of the worldwide coverage with broadband services and other scientific missions, as well.

According to the worldwide coverage missions, their network architecture in space could be categorized into single-layer (one-shell) networks and multilayer networks. A single-layer network provides intercommunication between only satellites of the same altitude, whereas multilayer networks enable communications between satellites in different shells. Multilayer networking is more complex but is advocated for its flexibility in providing more sustainable global coverage, seamless handovers, and reliable communications.

LEO satellites used at the end of the past century were known as microsatellites because of their light weight and small dimensions. Later, nanosatellites were developed as more convenient structure for launching process, since less energy is required to launch such satellites into the LEO space slot. But recently, it has been possible to launch nanosatellites from the International Space Station (ISS) (List of spacecrafts deployed from the International Space Station 2020). Related to the launching process, LEOs play an additional role as the first space shell for the satellites toward geosynchronous (geostationary) orbits, due to the three-step transfer process (known as Hohmann transfer) (Cakaj et al. 2015a).

LEO satellites and appropriate ground platforms (access points) now represent a very useful system, not only for the main mission as communication is but also for research scientific missions. Through LEO satellites and appropriate platforms, anywhere on the globe can be provided data about the water dirtiness of the river Amazon, about new exoplanets, natural disasters, air or marine disasters, how the wheat is growing in South Africa, how many refugees are crossing the borders, ice melting, and increasing seawater level, for example.

Related to the last item, the satellite *Sentinel-6 Michael Freilich*, launched on November 21, 2020, from Vandenberg launching site in California and consolidated into the LEO orbit of altitude of 1336 km under 66^0 inclination, will measure the sea level around the globe for the next five years. The mission is collaboration between NASA and the European Space Agency (see Figure 1.1) (Sentinel-6 Michael Freilich 2021).

Finally, as the nineteenth century was deeply marked with the steam machines, this century will be marked by LEO satellites, hopefully for the better life on Earth! These tools provide opportunities not only for communications but also for scientific purposes, including Earth and space observation. LEO satellites serving as "eyes" in the sky might also prove useful for world peace!

Figure 1.1 *Sentinel-6 Michael Freilich* spacecraft.

Communication with such missions is enabled through the ground stations; thus, the performance of the ground station is crucial for such missions, and will be elaborated on throughout this book.

1.2 Satellite System Architecture

The scheme of a typical satellite communication system architecture is shown in Figure 1.2 (Maral and Bousquet 2005). It includes a ground segment, space segment, and control segment.

The operational satellite receives the radio waves transmitted by the ground station. This is called *uplink*. The received signals by satellite are processed, translated into another radio frequency, and amplified on-board. In turn, these signals are further transmitted to the receiving ground station. This is called *downlink*. Uplinks and downlinks are based on radio frequency modulated carriers' principles. Carriers are modulated by baseband signals, including analog or digital, conveying information for communication or for other purposes.

The *space segment* contains one or several active and spare satellites organized in a constellation. The satellite is an artificial body orbiting around the Earth as "flying" trans-receiver, either for communication or scientific purposes. Each satellite consists of a *payload* and *platform* (bus). The *payload* consists of the receiving and transmitting antennas and all electronics that support the reception and the transmission of radio carriers. The satellite's payload has two main functions:

To amplify the received carriers for retransmission to the downlink. Large distance between the ground station and the satellite causes the carrier's power at the input of the satellite's receiver to be too low. Thus, power must be amplified to feed the satellite's transmit antenna toward users on ground within its coverage area.

Frequency conversion. Frequency conversion is required to increase isolation between the receiving input and transmitting output (avoiding the re-injection into the receiver). In Figure 1.3, the transparent satellite payload is given, making clear the uplink/downlink isolation.

Transparent payload belongs to a single antenna beam satellite where each transmit and receive antenna generates only one beam. Figure 1.3 shows that carriers are power amplified, and frequency

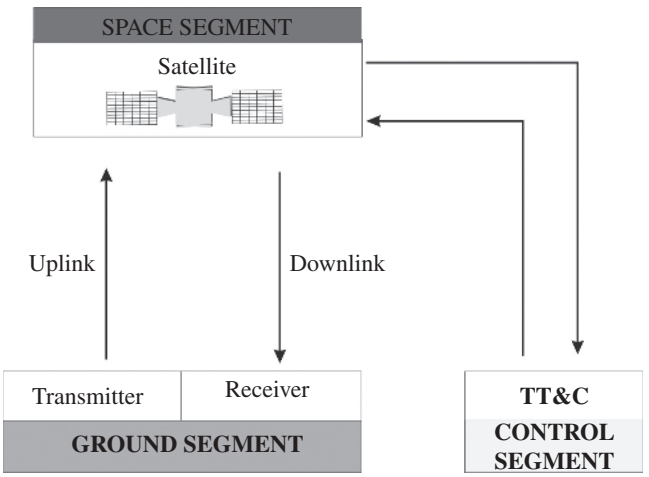

Figure 1.2 Typical satellite communication system architecture.

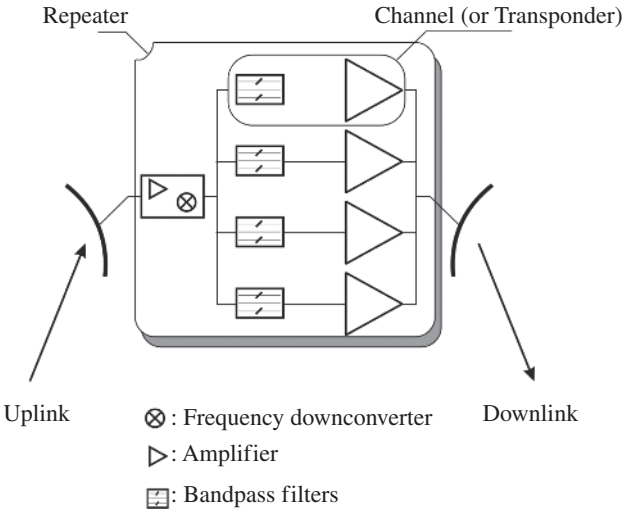

Figure 1.3 Transparent payload.

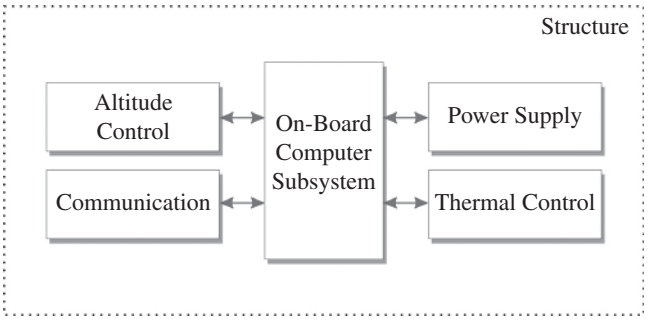

Figure 1.4 Satellite platform block scheme.

down converted. The amplifying chain associated with each sub-band is called *satellite channel* or *transponder*. The bandwidth splitting is achieved using a set of filters. Regenerative payload (multibeam) antennas would have many inputs/outputs as up beams/down beams. Routing of carriers from one up beam to a given down beam implies on-board switching at radio frequency. LEO satellites for scientific purposes usually use single-beam antennas.

The satellite *platform* consists of subsystems that permit the payload to operate. These subsystems are: structure, power supply, temperature control, altitude control, and communication subsystem (see Figure 1.4).

The structure provides the necessary mechanical support. The electrical power supply subsystem provides the necessary DC power. The altitude control subsystem stabilizes the satellite and controls its orbit. The thermal control system maintains the temperature of various subsystems within tolerable limits. All these functions are controlled by on-board computerized subsystem.

Some missions, in principle, can be realized just by a single satellite, but for real-time continuity of services and large or full Earth's coverage, the space segment must be organized as single-layer or multilayer constellation. A single-layer network provides intercommunication between only satellites of the same altitude, whereas multilayer networks enable communications between satellites in different orbital shells. Multilayer networking is more complex, but it is more preferable.

Figure 1.5 One Web's segment of single shell network.

Active satellite projects related to an integrated satellite-terrestrial communications network include the Iridium constellation with 66 satellites (Cochetti 2015), the OneWeb constellation with 648 satellites (De Selding 2015; Pultarova and Henry 2017), Amazon, which has filed to launch 3,236 spacecrafts in its Kuiper constellation (Sheetz 2019), and Telesat, with the initiative of having a 117-spacecraft constellation (Foust 2018). Figure 1.5 illustrates a segment of OneWeb's existing network showing its longitudinal orbit planes (Constellation One Web 2022).

In my view, the most serious activities have been taken by SpaceX, whose *Starlink* constellation is planned to consist of thousands of small LEO satellites, deployed in three shells (layers), dedicated to maximizing broadband internet services toward global Earth coverage, and combined with ground stations (trans-receivers), to be organized as a satellite-terrestrial integrated network for real time worldwide broadband services. The *Starlink* single layer constellation at altitude of 550 km is given in Figure 1.6 (The real benefit of SpaceX-*Starlink,* highspeed internet, 2022).

The *ground station* is the location on the ground equipped with appropriate equipment to be used for communication with the satellite. The function of a ground station is to receive or transmit the information from/to the satellite in the most reliable manner while retaining the desired signal quality at the destination. Scientific missions can be accomplished in principle by only one ground station. The reason behind building more ground stations is to increase the coverage and number of measurements per observed objects or area, and practically increase data download capability. The communication between the satellite and a ground station is established when the satellite is consolidated in its own orbit, and it is visible from the ground station.

The ground segment consists of all the ground stations. These stations are most often connected to the end user equipment by a terrestrial network. Stations are distinguished by their size, which varies according to the volume of traffic to be carried and the type of traffic (voice, video, or data). Ground stations have experienced a tremendous reduction in size. The largest ground stations are equipped usually with antennas of 30 m diameter (Standard A of the INTELSAT network). The smallest ground stations have typically 0.6 m antennas (direct television receiving stations). Some stations both transmit and receive, and some of them are just receive-only (RCVO) stations.

The general organization of a ground station consists of antenna subsystem with associated tracking system, transmitting and receiving equipment, monitoring system, and normally power supply.

Figure 1.6 Starlink satellite single shell constellation at altitude of 550 km.

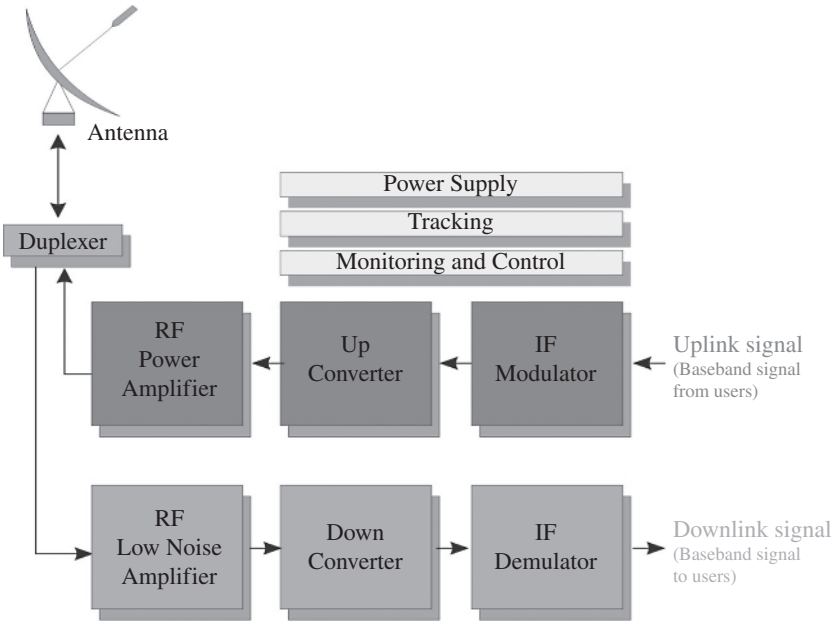

Figure 1.7 The architecture of a typical satellite ground station.

Figure 1.7 shows typical architecture of a ground station for both receiving and transmitting branches. This is a single antenna system where the uplink and downlink separation is achieved by duplexer (Cakaj and Malaric 2007a).

The *control segment* consists of all ground facilities for the control and monitoring of the satellites. This is known as Tracking, Telemetry & Command (TT&C).

1.3 The Satellite Ground Station

Ground stations are vital elements in any satellite communications network. Generally, they serve as an interface for communication between the satellite and different customers. The function of a ground station is to receive information from, or transmit information to, the satellite in the most cost effective and reliable way, while retaining the desired signal quality.

Depending on the applications, the ground stations may have both transmit and receive capabilities or may only be capable of either transmission or reception. Further categorization can be based on the type of services. Usually, the design criteria are different for the Fixed Satellite Service (FSS), the Broadcast Satellite Service (BSS), and Mobile Satellite Service (MSS).

Further concern is related to the ground stations dedicated for LEO satellites. The complexity and size of these ground stations depends on applications. The communication between the satellite and the ground station for scientific missions is usually established on S-band. The main characteristic of this type of stations, is that LEO stations employ tracking antennas to utilize the full capacity, since the satellite flies too fast over the ground station and having too short communication (usually less than 15 minutes) with the appropriate ground station, so the ground station antenna must follow the satellite with the high accuracy.

Thus, even though the communication or the goal of the mission can be accomplished with only one ground satellite station, because of the redundancy and to increase the download data capability, usually more ground stations are used for a single scientific satellite's mission. It is better if there is no overlap between two or more ground stations. The none-overlapping case is presented in Figure 1.8, related to the MOST (Microvariability and Oscillation of Stars) satellite which had ground stations in Canada (Toronto and Vancouver) and in Austria (Vienna) (Northern Lights Software Associates 2003; Keim et al. 2004).

Figure 1.8 shows that the stations in Vancouver and Toronto are overlapped but not with the Vienna ground station; therefore, the stations in Canada and the station in Vienna do not communicate with the LEO satellite at the same time. This increases the download data capability.

The quality of communication depends on the performance of the satellite ground station. Before implementing a satellite ground station, the analysis related to environmental factors must be considered, especially in urban areas. Rain effects, uplink and downlink antenna isolation, intermodulation interference, desensiblization, and analysis related to the contact time duration under

Figure 1.8 Visibility of the MOST satellite.

the low elevation angles are a few aspects treated within this work related to the final decision on design and implementation of the ground station. Most of the satellite services (among them scientific satellites) use frequency bands that are shared with terrestrial services. For systems to coexist, the ITU have specified certain constraints in the transmitted EIRP from the satellite. Such constraints have impact on the design of a ground station. Several trade-offs are necessary in the optimization process up to final design concept of the ground station.

A fundamental parameter in describing a ground station performance is *Figure of Merit* as a ratio of receiving antenna gain to system noise temperature (G/T_S). This Figure of Merit represents the sensitivity of the ground station. A higher value implies a more sensitive station.

The ground station can be considered as two subsystems, the transmit and receive subsystem. From this view, the ground station can be categorized as single antenna or double antenna system. For a single antenna configuration, the antenna is the common element for both subsystems. The transmit subsystem consists of several major components: baseband equipment, modulator, frequency upconverter, high-power amplifier (HPA), and antenna feed system. The receive subsystem behind the antenna feed system uses the low noise amplifier (LNA), frequency downconverter, demodulator, and baseband equipment. A general configuration of a single antenna ground station is shown in Figure 1.9 (Richharia 1999). Signals from the terrestrial network or directly from the user in some applications are fed to a ground station via a suitable interface. The baseband signals are then processed, modulated, and up-converted to the desired satellite transmit frequency. After up-conversion, the signals are amplified by HPA to the required level and transmitted via the antenna.

Signals received through antenna are amplified by LNA, then down-converted to an intermediate frequency (IF), demodulated, and transferred to the terrestrial network via an interface (or directly to the user in some applications). The feed system provides the necessary aperture illumination, introduces the required polarization, and provides the isolation between the transmitted and received signals. Other subsystems such as tracking, control, monitoring, and power supply provide the necessary support. Drive motors enable the ground station's antenna movement to follow the satellite above the ground station. The exact configuration of a ground station depends on applications. To illustrate this, in Figure 1.10 the configuration of the ground station implemented in

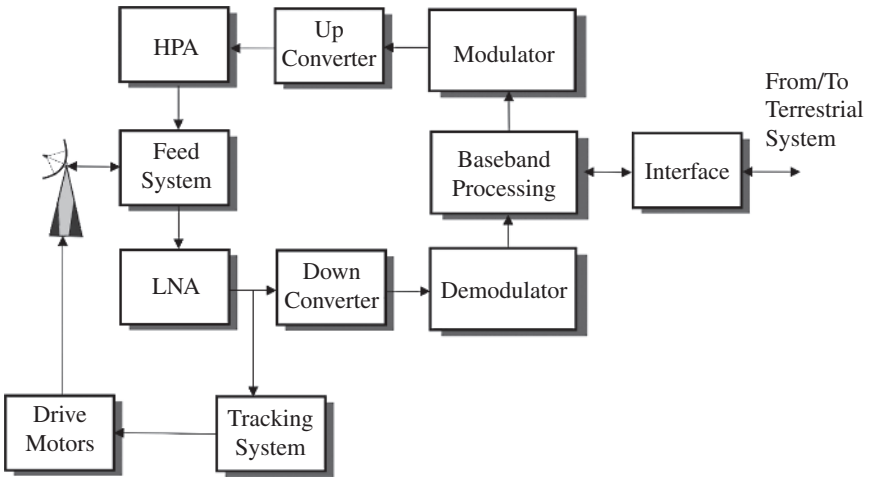

Figure 1.9 General configuration of a single antenna ground station.

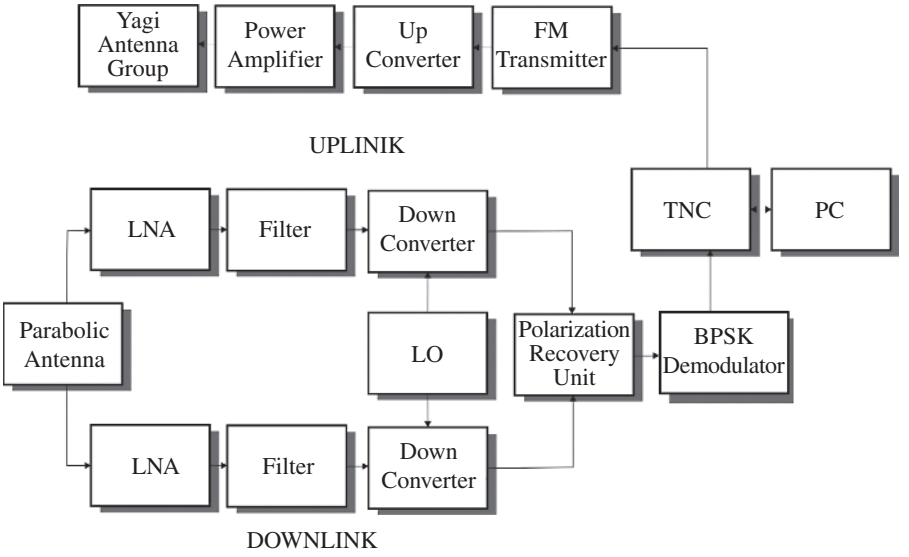

Figure 1.10 Block diagram of the Vienna LEO satellite ground station.

Vienna for communication with MOST satellite is presented, as a double antenna system configuration (Keim and Scholtz 2006). The Vienna ground station system was set up at the Institute for Astronomy of the University of Vienna in cooperation with the Institute of Communications and Radio-Frequency Engineering of the Vienna University of Technology. The Vienna LEO ground station achieved successful two-way communication with the MOST microsatellite on September 30, 2003, until March 2019, when the MOST satellite was deactivated (MOST-A tiny satellite probes the mysteries of universe, 2019). The acronyms in the Figure 1.10 are: BPSK (binary phase shift keying), FM (frequency modulation), LNA, LO (local oscillator), TNC (terminal node controller), and PC (personal computer).

The uplink block is planned to issue commands for: operating the satellite's payload, altitude control subsystem, and other housekeeping functions. The downlink block is responsible for receiving download observation data. The signal from the satellite is picked up by means of a parabolic antenna (diameter of 3 m), receiving two orthogonal polarization states, horizontal and vertical. The signal is amplified first by LNA and further by downconverters. To avoid possible blocking of downconverters due to stray coupling of the uplink transmit signal (full-duplex mode), filters are introduced between LNAs and downconverters.

The two-stage amplification by LNAs and low-noise converters is necessary to guarantee that the signal input to the demodulator will be sufficiently strong. A polarization recovery unit optimally combines the 140 MHz outputs of the two downconverters, choosing the higher output signal. A BPSK demodulator using FEC (forward error correction) recovers the received data signal. At the TNC, the transmit protocol will be removed.

The data collected from the satellite is stored at the appropriate storage device. At the uplink, the TNC adds the transmit protocol to data commands originated from the PC. A separate Yagi antenna group supports the uplink. The uplink signal is generated by means of a 435 MHz FM (frequency modulation) transmitter and then converted by upconverter at 2055 MHz. A power amplifier is placed near the antenna to avoid cable loss. Then, the transmit signal is transmitted via Yagi antenna group toward the satellite (Keim and Scholtz 2006).

1.4 Ground Station Subsystems

The most common ground station subsystems are:

- At the downlink: antenna, low noise amplifier, down converter, and demodulator
- At the uplink: the modulator, upconverter, high-power amplifier and antenna (Figure 1.7)
- Support safety system

These are described next.

1.4.1 Antennas

Because of the large signal attenuation at RF frequencies, the ground station antenna must have high signal gain and must be highly directional to focus power to and from the satellite. Most ground stations use parabolic reflector antennas since such antennas can readily provide high gain and the desirable side lobe characteristics. If the same feed is used for both polarizations, the feeder should separate and combine polarizations in a dual-polarized system. Table 1.1 provides a few typical parameters that should be considered for link budget calculations.

Generally, to avoid combiner (duplexer) loss, at the front-end separate antennas should be used for uplink and downlink, as a double antenna system configuration. The decision on the final antenna system design should be based on required downlink margin. The uplink and downlink antennas must be isolated from each other (Cakaj and Malaric 2007b).

LEO ground stations use tracking antennas, so an antenna mount is also required. The most used mount is *azimuth-elevation mount*, which provides azimuth and elevation angles control. The power control electronics provides the drive signals for the antenna tracking motors. The antenna pointing angle coordinates are precomputed for a satellite pass in the control computer based on the satellite's space orbital parameters. These coordinates are uploaded to the antenna control processor prior to a satellite pass. During a satellite pass, the antenna control processor commands the power electronics module, which positions the antenna in angular alignment with a satellite. The antenna position is updated frequently, depending on the mission's required accuracy (Reisenfeld et al. 2007).

1.4.2 Low Noise Amplifier

The weak signals at the downlink from the satellite are received by the parabolic antenna and then amplified by LNA. Table 1.2 provides some typical technical parameters for link budget calculations and implementation.

Table 1.1 Some of technical antenna's parameters.

Operating frequency	**1.0–12**	**GHz**
Gain at operating frequency	35	dBi
Diameter	3	m
Side lobes	–20	dB
Front/back ratio	–25	dB

Table 1.2 Some of technical LNA's parameters.

Operating frequency	2–2.5	GHz
Gain	30	dB
Noise figure	0.6	dB
Operating voltage	12	V

In case of double antenna system, due to coupling between transmitting and receiving antenna, the downlink antenna will also receive the transmitted signal (Cakaj and Malaric 2007b). In this case, filters should be used that efficiently suppress the transmit signal but do not introduce significant loss at the receiving frequency. The isolation between downlink and uplink for the double antenna system should be measured to be kept under allowable limits.

1.4.3 Converters

Up and down converters provide the translation between intermediate frequency (IF), which is typically 70 MHz or 140 MHz, and the actual uplink and downlink frequencies, respectively. The output power level from the downconverter should be sufficient to stimulate a demodulator, and the output power level from the upconverter should be sufficient to drive the power amplifier. In large or professional ground stations, the converters are separate units designed for flexibility, easy for maintenance, and stable operation. Table 1.3 provides typical technical parameters that should be considered for link budget calculations and implementation for converters. The typical downconverter and upconverter block diagrams used in satellite ground stations are presented in Figure 1.11 under a, b respectively (Elbert 1999).

A typical upconverter amplifies the signal to provide adequate gain for the operation of the station equipment. The actual frequency conversion is accomplished in a mixer and LO (local oscillator) combination such as shown in Figure 1.11. A frequency agile upconverter employs a frequency synthesizer to generate the LO so any carrier frequency within the satellite uplink band

Table 1.3 Some of technical converters' parameters.

Input frequency	2232	MHz
Local oscillator frequency	2372	MHz
Output frequency	140	MHz
Gain	32	dB
Noise figure	0.8	dB
Maximum input power	17	dBm
Output power	30	dBm
Spurious signal attenuation	40	dBc
Operating voltage	12	V

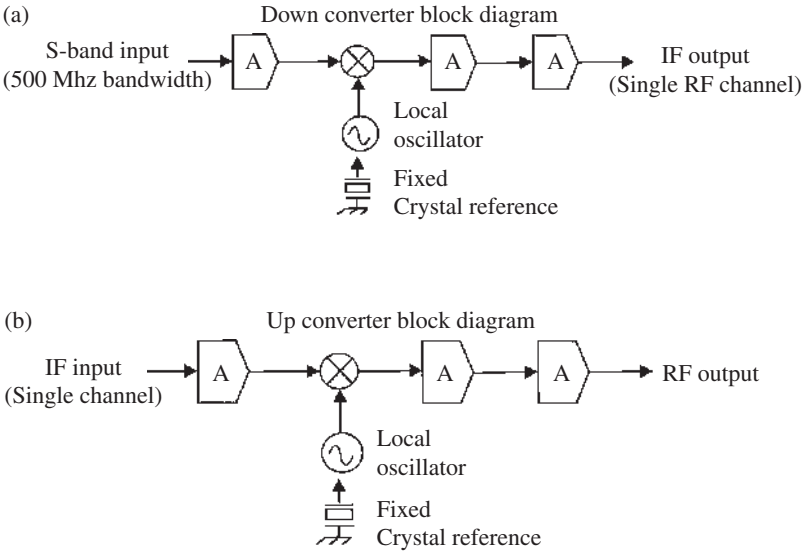

Figure 1.11 Upconverter and downconverter diagrams for satellite ground station.

can be used. Proper filtering is needed to prevent the LO and its harmonics from reaching the uplink path (Elbert 1999).

The downconverter is positioned behind the LNA. The first amplifier stage provides the needed overall gain and reduces the noise contribution of mixer and IF equipment. A synthesizer also must be used to provide agility in the receiving frequency operation (Elbert 1999).

1.4.4 Safety System

LEO satellites establish the lock with the ground station 6–8 times per day for 5–15 minutes at a time. These contacts are established both day and night. Thus, data should be automatically downloaded at the ground station because there will likely be times the station is unattended. The concept of an unattended ground station for LEO missions has been validated by the successful demonstration of a telemetry received terminal in the 2210–2295 MHz band (S-band) that tracked two NASA spacecrafts in LEO (Golshan et al. 1996). Successful demonstrations of the automated, unattended operations of the terminal were conducted with the Solar, Anomalous and Magnetospheric Particle Explorer (SAMPEX) in July and with the Extreme Ultraviolet Explorer (EUVE) in December 1994. Validation of demonstration was accomplished in December 1995 (Losik 1995). A safety/security system must be in place when using an automatic working mode. In principle, this system consists of two elements: storm safety system and visual monitoring system.

Storm safety system is designed to protect the antenna (dish), and the hardware structure from damages due to strong wind (see Figure 1.12). If the wind speed as measured with an anemometer exceeds certain a wind limit (for example of 70 km/h), then the rotator controller will react and the antenna will be brought to an elevation angle of 90° (zenith). In this position, it is protected, since the antenna has the smallest target area for the wind regardless of wind direction (Keim and Scholtz 2006). This is known as *antenna parking position*.

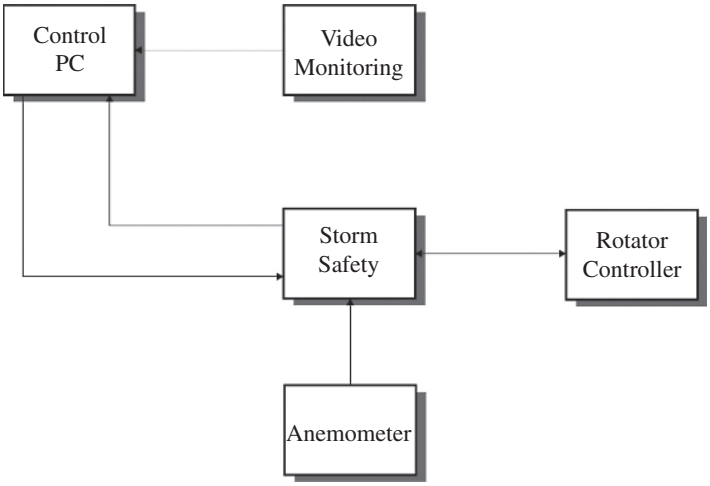

Figure 1.12 Block scheme of safety system.

1.5 Downlink Budget

A communication satellite system enables the communication between a satellite and one or more ground stations. The links used for interconnections should be designed to deliver the information at the destination with acceptable desired signal power level, according to the customer's requirements. A compromise is exercised between the quality of delivered information and practical constrains related to the propagation and the cost/quality of the equipment (Sklar 2005).

The performance of a communication satellite system is mainly expressed in a link budget. Factors that need consideration in a link design are operational frequency, propagation effects, terminal complexity, noise effects, and regulatory requirements. Usually, the costumers of the satellite communication systems in advance define their requirements related to the quality level that the system must fulfill. To satisfy and complete these costumers' requirements, a link power budget should be analyzed and completed. The link budget is a balance sheet of gains and losses; it outlines the detailed participation of transmission and reception resources, noise sources, and all effects throughout the link. The link budget includes both uplink and downlink.

Together with other modeling techniques, the link budget can help to predict equipment, technical risk, performance, and the cost. It is a tool for adjusting the ground station and satellite parameters to satisfy the requirements on the optimal way. An accurate link budget includes many parameters, such as the following (Gordon and Morgan 1993):

- Antenna gain (G)
- Equivalent Isotropic Radiated Power ($EIRP$)
- Free space loss (L_S)
- System noise temperature (T_S)
- Figure of Merit for receiving system (G/T_S)
- Link margin (LM)

1.5.1 Error-Performance

In general, for digital communications, *the error performance* is expressed through E_b/N_0 where E_b is bit energy and N_0 is noise power spectral density (Sklar 2005). Bit energy E_b can be written as:

$$E_b = ST_b \tag{1.1}$$

where S is the signal power and T_b determines the time occupied by a single bit. Also, $N_0 = N/B$ where N is noise power and B is a bandwidth. The bit time T_b is reciprocal with bit rate R_b, and then the error performance can be displayed as:

$$\frac{E_b}{N_0} = \frac{S}{N}\frac{B}{R_b} \tag{1.2}$$

The Eq. (1.2) tells us, that the analysis of error performance of digital communication system can be done through analysis of S/N (signal-to-noise ratio), which is very common from analogue systems. This ratio refers to average signal power and average noise power. The higher the signal-to-noise ratio, under the fixed bandwidth and the fixed bit rate, the better is the energy bit over noise density ratio.

The ratio S/N can degrade by two reasons:

- Through the decrease (loss) of the desired signal power (S)
- Through the increase of the noise power (N)

Furthermore, we will call these degradations, respectively, *loss* and *noise*. Losses are:

- *Free space loss* is a decrease of the wave's power simply as a function of distance. For a satellite communication link, the free space loss is the largest loss because of the long distance between transmitting and receiving terminals.
- *Atmospheric loss* includes all effects of atmosphere with the influence on decrease of the signal power.
- *Polarization loss* is a loss of signal due to any polarization mismatch between the transmitting and receiving antennas.
- *Pointing loss* is a loss of signal when either the transmitting antenna or receiving antenna is imperfectly pointed.
- *Noise* has several sources along signal's route such are: thermal, atmospheric, galaxy, and interference from other sources.

1.5.2 Received Signal Power

The main purpose of the link budget is to verify that the communication system will operate according to the predicted-designed plan. This means that the error performance will meet the specifications. In radio communication systems, the carrier power is propagated from the transmitter using transmitting antenna, which will then be received through receiving antenna. The development of the fundamental relationship between transmitted and received power usually begins with the assumption of an omnidirectional RF (radio frequency) source, transmitting uniformly over 4π steradians. Such an ideal source, called an isotropic radiator, is illustrated in Figure 1.13 (Sklar 2005).

The power density $p(d)$ on a hypothetical sphere at the distance d from the source is related to the transmitted power P_t as:

$$p(d) = \frac{P_t}{4\pi d^2} \tag{1.3}$$

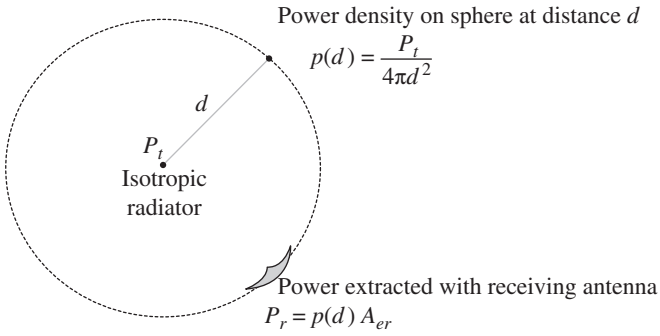

Figure 1.13 Received power from an isotropic antenna.

where $4\pi d^2$ is the sphere's area. The extracted power with the receiving antenna will be:

$$P_r = p(d)A_{er} \tag{1.4}$$

$$P_r = \frac{P_t A_{er}}{4\pi d^2} \tag{1.5}$$

where P_r is received power and A_{er} is the absorption cross section (effective area) of the receiving antenna. The parameters without index are general for both. An antenna's effective area A_{er} and physical area A_p are related by an efficiency parameter as:

$$A_{er} = \eta A_p \tag{1.6}$$

which clarifies that total incident power is not extracted. Values of η are in range from 0.4 to 0.8 but the most common value is $\eta = 0.55$ (Sklar 2005). Further, all parameters related to transmission terminal will be designated by index t and to receiving terminal by index r.

The effective radiated power or *equivalent isotropic radiated power* (*EIRP*) with respect to an isotropic source is defined as a product of transmitted power P_t and the gain of the transmitting antenna G_t, as follows:

$$EIRP = P_t G_t \tag{1.7}$$

However, for the more general case in which the transmitter has an antenna gain relative to an isotropic antenna, the P_t in Eq. (1.5) can be replaced with $P_t G_t$ or with EIRP. Based on Eq. (1.7), then, Eq. (1.5) becomes

$$P_r = EIRP \frac{A_{er}}{4\pi d^2} \tag{1.8}$$

The relationship between antenna gain G and antenna effective area A_{er} is:

$$G = \frac{4\pi A_{er}}{\lambda^2} \tag{1.9}$$

where λ the wavelength of the carrier is. Wavelength λ and frequency f are related by Eq. (1.10),

$$\lambda = \frac{c}{f} \tag{1.10}$$

where c is the light's velocity (considered as $c = 3 \cdot 10^8$m/s).

The expression in Eq. (1.9) is similar for both transmitting and receiving antennas. The *reciprocity theorem* states that for a given antenna and carrier wavelength, the transmitting and receiving gains are identical. All discussion is done under assumption of an isotropic source, and then the antenna gain is $G = 1$. Putting this at Eq. (1.9) yields

$$A_{er} = \frac{\lambda^2}{4\pi} \tag{1.11}$$

To find the received power P_r when the receiving antenna is isotropic, we substitute Eq. (1.11) at Eq. (1.8) to get

$$P_r = \frac{EIRP}{(4\pi d/\lambda)^2} = \frac{EIRP}{L_S} \tag{1.12}$$

where collection of terms $(4\pi d/\lambda)^2$ is known as *free space loss* designated by L_S.

$$L_S = \left(\frac{4\pi d}{\lambda}\right)^2 = \left(\frac{4\pi df}{c}\right)^2 \tag{1.13}$$

For the more general case, when the receiving antenna is not isotropic, this means it has an antenna gain G_r. The Eq. (1.12) becomes more general, as:

$$P_r = \frac{(EIRP)G_r\lambda^2}{(4\pi d)^2} = \frac{(EIRP)G_r}{L_S} \tag{1.14}$$

The Eq. (1.14) shows that the received power depends on *effective radiated power*, *free space loss,* and *receiving antenna gain*. Usually, all above-mentioned parameters are expressed in (dB); however, the *equation* expressed in (dB) is:

$$P_r = EIRP - L_S + G_r \tag{1.15}$$

Free space loss is the greatest loss in transmitted power due to the long distance between the satellite and ground station. The free space loss L_S strongly depends on distance d and frequency f, as presented in in Figure 1.14.

The diagram is presented for frequencies of 2 GHz, 8 GHz, and 12 GHz and for distances from 1,000 km up to 36,000 km, including the highs related to LEO, MEO, and GEO orbits. Figure 1.14 shows that free space loss increases by both frequency and the distance. This has a large impact on transmitted signal power.

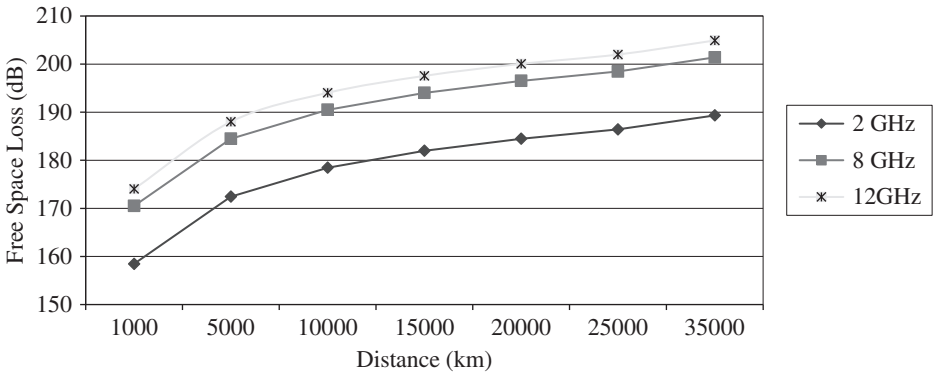

Figure 1.14 Free space loss.

1.5.3 Link Budget Analyses

Evaluating system performance, the previous analysis has shown that the quantity of the highest interest is $S/N(SNR)$, or signal-to-noise ratio. In satellite communication systems, mostly the carrier is frequency or phase modulated (frequency shift keying (FSK) or phase shift keying (PSK)), having a constant envelope. This means that the signal power and carrier power are the same; thus, the signal power will keep notation S. Then the ratio S/N can be obtained from Eq. (1.12), (1.14), divided by N as:

$$\frac{S}{N} = \frac{EIRP(G_r/N)}{L_S} \tag{1.16}$$

For digital communications systems, Eq. (1.16) is used to express this ratio by noise power spectral density. Thus, applying $N_0 = kT_s$ yields:

$$\frac{S}{N_0} = \frac{EIRP(G_r/T_S)}{kL_S} \tag{1.17}$$

where T_S is system noise temperature, representing the noise radiated into antenna and thermal noise generated by the receiving system. L_S is free space loss. The system effective noise temperature T_S is a parameter that models the effects of various noise sources. The ratio G_r/T_S is known as a Figure of Merit. The Eq. (1.17) expressed in (dB) follows:

$$\frac{S}{N_0} = EIRP - L_S + G_r/T_S + 228.6 \tag{1.18}$$

In this equation the value of $228.6dBW/HzK$ yields from Boltzmann's constant. The signal to noise power expressed as logarithmic equation is:

$$\frac{S}{N}(dB) = \frac{S}{N_0}(dB) - B(dB) \tag{1.19}$$

Within link budget calculations, the atmospheric losses and other degradation factors that affect the received power must be considered. Then, if we introduce the term L_0, which represents all other loss factors, and apply it at Eq. (1.18), expressed in dB, we'll get:

$$\frac{S}{N_0} = EIRP - L_S - L_0 + G_r/T_S + 228.6 \tag{1.20}$$

known as the *range equation*.

The downlink margin (DM) is defined as:

$$DM = \left[\frac{S}{N}\right]_r - \left[\frac{S}{N}\right]_{rqd} \tag{1.21}$$

where r indicates the expected signal-to-noise ratio to be received at receiver, and rqd means required signal to noise ratio by customer, based on in advance defined performance. So, a positive value of DM is an indication of a good system performance. To guarantee a positive link margin, we must trade among parameters of range equation. If all the parameters of the link are rigorously treated (the worst case), high link margin is not mandatory.

Thus, in principle the needed items to calculate signal power over noise power density are $EIRP$, G_r/T_S, and (L_S, L_0). $EIRP$ is the power transmitted from the satellite, and it does not depend on environmental factors. G_r is receiving antenna gain. Other loss includes atmospheric, polarization,

and pointing loss. The atmospheric impairments are analyzed latter on, and the pointing loss can be avoided by accurate pointing equipment. Of further interest remain free space loss and system temperature.

Since LEO satellites move too fast over the Earth, the satellite's slant path range (distance in between the ground station and the satellite) varies over the time, on dependence of the elevation angle, so, the signal toward the ground station is faced with different distances from the satellite to the ground station, and consequently different free space loss under different elevation. The variation on free space loss under different elevation impacts signal-to-noise spectral density ratio, and consequently the receiving ground station performance. The following equation expresses the dependence of free space loss on the elevation angle under which one the ground station sees the satellite:

$$L_s(\varepsilon_0) = \left(\frac{4\pi f}{c}\right)^2 d^2(\varepsilon_0) \tag{1.22}$$

The next sections of this chapter will discuss the system temperature, followed by satellite ground station geometry.

1.6 Figure of Merit and System Noise Temperature

For the satellite communication system, the performance of the receiving system, or known as the downlink performance, what is the subject of this book, is commonly defined through a receiving system Figure of Merit as G/T_S, where:

$$T_S = T_A + T_{comp} \tag{1.23}$$

Here, G is receiving antenna gain, T_S is receiving system noise temperature, T_A is antenna noise temperature and T_{comp} is composite noise temperature of the receiving system, including lines and equipment. The composite temperature depends exclusively on parameters of technical equipment and of interconnection lines characteristics. Otherwise, the antenna temperature T_A depends on external environment factors also including the sky background represented by its sky noise temperature denoted as $T_{C.}$

Schematically, the satellite ground station receiving system and the environment concept is presented in Figure 1.15.

Unwanted noise power is, in part, injected via antenna (kT_AB) and part is generated internally ($kT_{comp}B$) by line loss and equipment. k is Boltzmann's constant and B is system bandwidth. T_c represents the sky noise temperature, T_m is medium temperature, and A is medium attenuation (Saunders 1993). Further will be discussed antenna noise temperature and composite noise temperature, both components of system temperature expressed by Eq. (1.23).

Different noise sources (natural, man-made, or interferences) at surrounding environment are present in the front of the receiving antenna of the satellite ground station system. The antenna will pick up part of this noise. The picked-up noise power from these external sources is given as kT_AB, where T_A is *antenna noise temperature*. The picked-up noise power depends on where the antenna is looking at. The antenna noise temperature is a measure of the effective temperature integrated over the entire antenna pattern.

In general, the total antenna noise power will be made up by the various sources whose temperature will vary with the space angle of observation (θ, ϕ). This power will be picked up by the

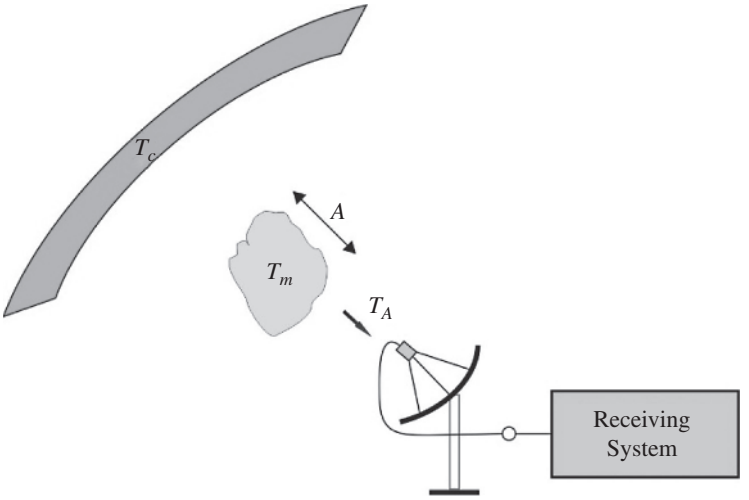

Figure 1.15 Satellite ground station and environment concept.

antenna, which power pattern is $F(\theta, \phi)$ (Saunders 1993; Nikolova 2002). Generally, antenna temperature can be expressed by:

$$T_A = \frac{1}{\Omega_A} \oint_{4\pi} \oint_{4\pi} F(\theta, \phi) \cdot T_C(\theta, \phi) d\Omega \tag{1.24}$$

where $T_C(\theta, \phi)$ is sky noise source temperature and Ω_A is antenna beam angle under which antenna sees this source. Sky noise temperature is generated from different sky sources (cosmic radiation, Sun, Moon, stars etc.), and the antenna adds internal noise to the receiving system; both degrade the downlink's performance.

The cosmic background radiation (D), presented in Figure 1.16, is independent of frequency and appears everywhere in the sky at the temperature of around 3–10 K. The galactic noise temperature by stars is also presented. The range of these variations is indicated as region (C). This noise decreases rapidly with frequency (Saunders 1993).

Considering that the entire antenna pattern (beam) sees a sky noise source under the same temperature conditions, then $T_C(\theta, \phi) = const = T_C$. This assumption is valid when the solid angle Ω_C

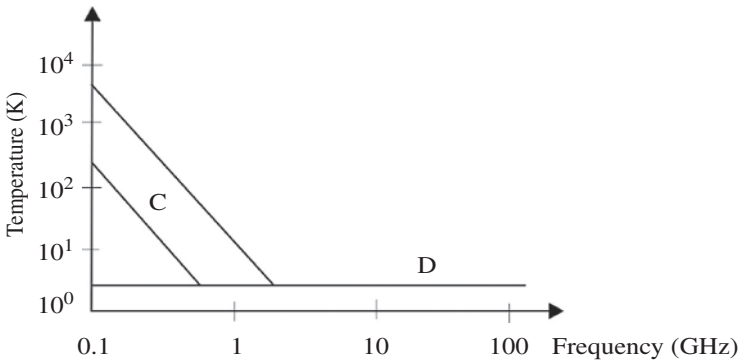

Figure 1.16 Sky noise temperature sources.

subtended by the noise source is much larger than the antenna solid angle Ω_A, which is the case for the receiving antennas at LEO satellite ground stations. Next, the antenna itself is considered lossless; it does not generate noise itself. Then, Eq. (1.24) becomes:

$$T_A = \frac{T_C}{\Omega_A} \oint_{4\pi} F(\theta, \phi) d\Omega \tag{1.25}$$

Since:

$$T_C(\theta, \phi) = const = T_C \tag{1.26}$$

and

$$\oint_{4\pi} F(\theta, \phi) d\Omega = \Omega_A \tag{1.27}$$

In case of $\Omega_A \ll \Omega_C$, yields out:

$$T_A = T_C \tag{1.28}$$

This means, that the antenna temperature T_A is equal to the sky source temperature T_C. From Figure 1.16 we see that for LEO satellites operating at 2 GHz band, sky noise temperature does not depend on galactic noise (region C), so it remains as constant within LEO satellites operating frequency range.

When an atmospheric absorptive process takes place (see Figure 1.15), the absorption increases the antenna noise temperature. If we consider the total cosmic temperature as T_C, the absorptive process (rain) medium temperature as T_m and the attenuation due the absorptive process as A, then the total antenna noise temperature T_A of the receiving satellite ground station is (Saunders 1993):

$$T_A = T_m\left(1 - 10^{-A/10}\right) + T_C 10^{-A/10} \tag{1.29}$$

where, typically T_m is 275 K to 290 K for rain. So, finally three components, two temperatures T_m, T_C and medium attenuation A will determine antenna noise temperature T_A.

Let us move to the second sum component, respectively, to the composite noise temperature T_{comp} analysis. Figure 1.17 presents the first stage of a satellite receiving system, including the elements where the loss and noise will have the primary role on S/N degradation. These elements are the antenna, line, and equipment (as the front-end device is the LNA). For calculations of the composite noise temperature equipment and line will be treated.

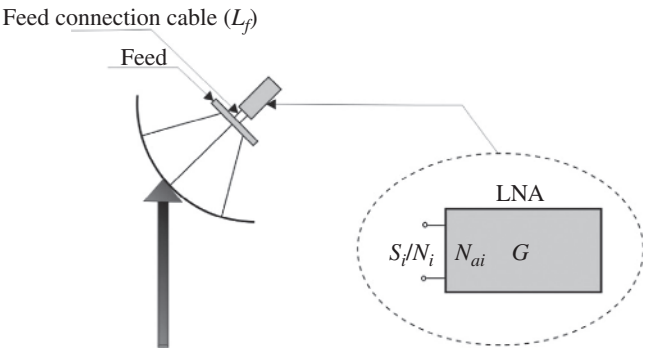

Figure 1.17 The first stage of a satellite receiving system.

Let us generally touch the *thermal noise*, where one degrades the signal-to-noise power ratio at the receiver. *Thermal noise* is caused because of thermal motion of electrons at physical temperature T. These motions of electrons generate the electromagnetic radiation. Part of this radiation in microwave frequencies will be present at the receiving system. The noise power spectral density N_0 is constant at all frequencies, known as *white noise*.

The noise power N within a bandwidth B is:

$$N = kTB \tag{1.30}$$

T is temperature in Kelvin (K), $k = 1.38 \cdot 10^{-23}$W/HzK is Boltzmann's constant.

The noise power spectral density N_0 (noise power within a bandwidth $B = 1$Hz) is:

$$N_0 = N/B = kT \tag{1.31}$$

From Eq. (1.31), the noise power density of thermal noise depends on the ambient temperature of the source. This leads to the useful concept of an *effective noise temperature* for noise sources that are not necessarily thermal in origin (e.g., galactic, atmospheric), which can be introduced into the receiving antenna. The noise power of such sources can be expressed separately through the effective noise temperature of a hypothetical thermal noise source power. The total effect of such noise sources, including external and internal, will be expressed through *system temperature*.

Noise figure is a parameter that expresses the noisiness of two port networks or devices (such as LNA). Noise figure F relates the S/N at the input of a network or device to the S/N at the output of the network or device. Noise figure of the preamplifier (LNA) at the receiving system shown in Figure 1.17 is defined as:

$$F = \frac{(S/N)_{in}}{(S/N)_{out}} = \frac{S_i/N_i}{GS_i/G(N_i + N_{ai})} \tag{1.32}$$

where S_i is signal power at the amplifier input port, N_i is noise power at the amplifier input port, N_{ai} is amplifier's internal noise referred to the input port and G is amplifier's gain. The Eq. (1.32) can be reduced to:

$$F = \frac{N_i + N_{ai}}{N_i} = 1 + \frac{N_{ai}}{N_i} \tag{1.33}$$

An ideal amplifier with no internal noise ($N_{ai} = 0$) has noise figure $F = 1$ or $F\,(\text{dB}) = 0$ dB. For the concept of the noise figure to have utility a value of N_i must be defined as a reference. The noise figure of any device then represents the measure compared with the reference value. In 1944, Fries suggested the noise figure should be defined for a noise source at a reference temperature of $T_0 = 290$K (Saunders 1993). From Eq. (1.31), it can be seen that the noise power spectral density from any source is characterized by appropriate noise temperature. The value of 290K is chosen as a reference because it is reasonable source temperature for many links. If substitutes $T = 290$K at Eq. (1.31) and expresses it in (dB) will have:

$$N_0 = -204\ (\text{dBW/Hz}) \tag{1.34}$$

By rearranging Eq. (1.33), we can write:

$$N_{ai} = (F-1)N_i \tag{1.35}$$

At Eq. (1.35) can be replaced $N_i = kT_0B$ and $N_{ai} = kT_RB$ where T_0 is the reference environmental temperature and T_R is called the effective noise temperature of the receiver (amplifier). Then the Eq. (1.35) becomes:

$$kT_RB = (F-1)kT_0B \tag{1.36}$$

$$T_R = (F-1)T_0 \tag{1.37}$$

Finally, for $T_0 = 290\text{K}$ we will get:

$$T_R = (F-1)\cdot 290\text{K} \tag{1.38}$$

or, typically for the LNA in Figure 1.17, is:

$$T_{LNA} = (F_{LNA}-1)\cdot 290\text{K} \tag{1.39}$$

Finally, the LNA noisiness expressed through noise figure F_{LNA}, is represented through LNA effective noise temperature. Thus, the noisiness of an amplifier is manifested through the noise temperature, what will further be seen how this approach mathematically simplifies the Figure of Merit calculations for LEO satellite ground station. The last equation tells us that the noisiness of an amplifier can be modeled as it was caused by a noise source, operating at some effective temperature $T_R(T_{LNA})$.

The next element in the Figure 1.17 is the line that connects the feed and LNA. Analyzing LNA, it was seen that S/N degradation resulted from injecting additional (amplifier's) noise into the link. However, in the case of line loss, the S/N degradation results from the signal being attenuated by the transmission line. Considering the line as a network where the line is matched with characteristic impedance at the source and at the load, we can define the power loss as:

$$L = \frac{P_{in}}{P_{out}} \tag{1.40}$$

Considering the network gain as $G = 1/L$, where L is the line loss, and applying the same methodology as for amplifier, we can find out that the *effective noise temperature for line loss* is:

$$T_L = (L-1)\cdot 290K \tag{1.41}$$

or, typically for the case in Figure 1.17, related to the interconnection line of the antenna feeder with LNA it is:

$$T_{Lf} = \left(L_f - 1\right)\cdot 290K \tag{1.42}$$

We have analyzed the noise temperature for a single device and for a single interconnection line, but in the real-world systems, there are more components interlinked to each other through more lines, linked as a chain (known as series or cascade interconnection). Each of them affects the system noise. The whole impact of devices and links within a system is defined as a *composite noise temperature*, including the effect of all equipment and lines. To analyze composite effect of all system components, we will first consider two networks interconnected in series with noise figures respectively F_1 and F_2 presented in Figure 1.18a (Sklar 2005).

Based on Eq. (1.32) and Eq. (1.33) as a definition for noise figure and simply mathematical operations, we can find out that the composite noise figure for these two networks is:

$$F_{comp} = F_1 + \frac{F_2 - 1}{G_1} \tag{1.43}$$

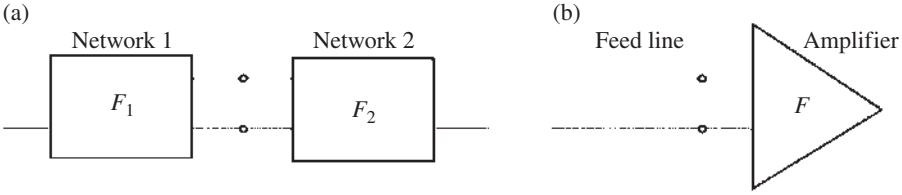

Figure 1.18 Networks connected in series.

where the G_1 is the gain of the Network 1. For the typical case, from the Figure 1.18b, are $F_1 = L_f$, $G_1 = G_f = 1/L_f$ and $F_2 = F_{LNA}$. Substituting these at Eq. (1.43) will get F_{comp} as:

$$F_{comp} = L_f + L_f(F_{LNA} - 1) = L_f F_{LNA} \tag{1.44}$$

Applying relation between F_{comp} and T_{comp} as:

$$T_{comp} = \left(F_{comp} - 1\right)290K \tag{1.45}$$

yields out:

$$T_{comp} = \left(L_f F_{LNA} - 1\right) \cdot 290K \tag{1.46}$$

The composite temperature can be displayed also as a function of effective noise temperature of the preamplifier (T_{LNA}) and of effective noise temperature of line loss (T_{Lf}) as follows:

$$T_{comp} = \left[\left(L_f - 1\right) + L_f(F_{LNA} - 1)\right] \cdot 290K = T_{Lf} + \frac{1}{G_f} T_{LNA} \tag{1.47}$$

To find out the composite noise figure F_{comp} and composite noise temperature T_{comp} of n networks, which are connected in cascades and characterized with F_n and G_n, the following equations apply:

$$F_{comp} = F_1 + \frac{F_2 - 1}{G_1} + \frac{F_3 - 1}{G_1 G_2} + \ldots + \frac{F_n - 1}{G_1 G_2 \ldots G_{n-1}} \tag{1.48}$$

$$T_{comp} = T_1 + \frac{T_2}{G_1} + \frac{T_3}{G_1 G_2} + \ldots + \frac{T_n}{G_1 G_2 \ldots G_{n-1}} \tag{1.49}$$

Finally, for the general case, to determine the Figure of Merit (G/T_S) for the satellite ground station, apply Eq. (1.23), (1.29), and Eq. (1.49), with respective parameters at each equation. Usually, the link budget is presented in the tabulated format, for both uplink and downlink with all appropriate parameters included the order of steps of their calculation given under Tables 1.4 and 1.5. In the following chapters practical calculations are provided.

Table 1.4 Downlink budget.

Transmit power	**dBW**
Loss	dB
Antenna gain	dBi
EIRP	dBW
Total propagation loss	dB
Received isotropic power	dBW
Antenna gain	dBi
System noise temperature	dBK
Figure of Merit (G/T_S)	dB/K
S/N_0	dB
Receiver bandwidth	dBHz
S/N	dB
Required S/N	dB
Downlink margin	dB

Table 1.5 Uplink budget.

Transmit power	dBW
Loss	dB
Antenna gain	dBi
EIRP	dBW
Total propagation loss	dB
Received isotropic power	dBW
Antenna gain	dBi
System noise temperature	dBK
Figure of Merit (G/T_S)	dB/K
S/N_0	dB
Receiver bandwidth	dBHz
S/N	dB
Required S/N	dB
Uplink margin	dB

1.7 Satellite and Ground Station Geometry

Theoretically, the position of the orbit is fixed in space, as for further analysis it is considered. The position of the satellite in space is determined by space orbital elements, in this order, the position of the orbital plane in space (orbit lays on orbital plane) is defined in reference to the Vernal equinox and equatorial plane, further the position of the orbit within its orbital plane is determined by argument of perigee (referred to line of nodes), and further the position of the satellite within its orbit is determined with its true anomaly angle (referred to the perigee) (Cakaj et al. 2007c).

As the satellite orbits, the Earth where the ground station sits rotates as well. Because of this, the distance between the ground station and the satellite changes over time, for LEOs and MEOs. Since LEOs move faster, these variations in distance between the satellite and ground station happen faster than under the case with MEOs. This is not the case with GEOs, since the orbit is synchronized with the Earth's rotations and thus the distance between the ground station and the satellite will not change under normal conditions.

The main goal of the satellite systems is establishing the communication between the satellite and the ground station. The location of the ground station is usually given in terms of geographical coordinates defined as *latitude* and *longitude*. Thus, for link budget calculation (which enables the communication by providing sufficient signal to noise level), correlation between the satellite position and the ground station location should be established, and mathematically expressed. This in fact brings the problem on finding out the slant range in between the ground station and the satellite, for the look angles under which the satellite is seen from the ground station. But how is the satellite seen from the ground station?

The position of the satellite within its orbit considered from the ground station point of view can be defined by *azimuth* and *elevation* angles. The horizon plane for a given ground station is depicted in Figure 1.19, to define the concepts of *azimuth* and *elevation*.

The *azimuth* (A_z) is the angle of the direction of the satellite, measured in the horizon plane from geographical north in clockwise direction. The *elevation* (ε_0) is the angle between a satellite and the

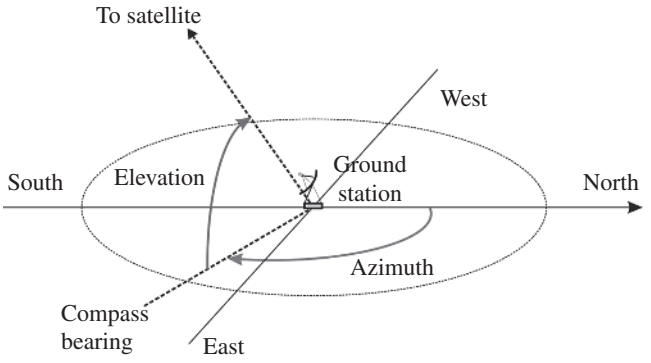

Figure 1.19 Azimuth and elevation.

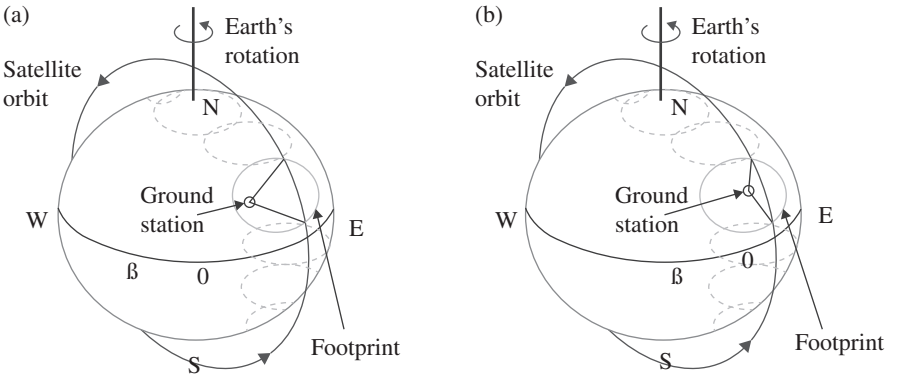

Figure 1.20 Satellite passes for an Earth rotation angle of β per orbit.

observer's (ground station) horizon plane. These two quantities are of primary interest for pointing a tracking antenna at LEO ground station to the satellite.

LEO satellites, being closer to the Earth, orbit several times daily around the Earth. Because of the Earth's motion around its north–south axis the satellite passes related to the determined ground station change from pass to pass. The orbital plane is in principle fixed and defined by orbital parameters, so the orbit keeps its position unchanged, but because of Earth's rotation around its N-S axis for angle β the ground station changes the position relatively to orbital plane, so the pointing (look angles) from the ground station to the satellite are not identical at both passes, for the same satellite's orbital position in space (Figure 1.20a,b) (Roddy 2006). This is illustrated in Figure 1.20.

To further clarify the correlation between the satellite and the ground station location, more exactly to find out the distance between the ground station and the satellite, in Figure 1.21 the position of a satellite within inclined orbital plane (LEO) with respect to the ground station is presented.

In Figure 1.21 both the satellite radius vector $\vec{r}$ and the ground station radius vector $\overrightarrow{R_E}$ for any position of the satellite and the ground stations are known. From the Figure 1.21 yields:

$$\vec{d} = \vec{r} - \overrightarrow{R_E} \tag{1.50}$$

$\vec{d}$ is the satellite to ground station range vector.

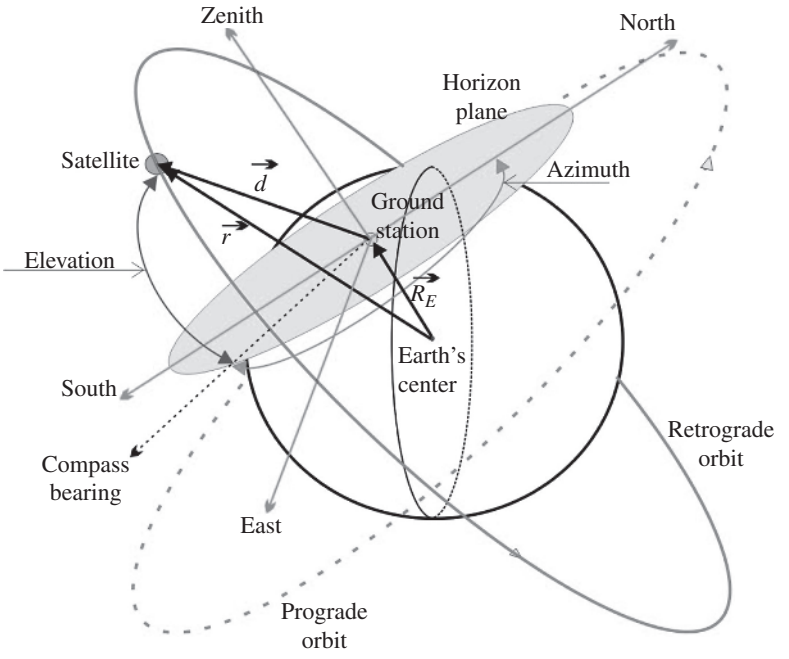

Figure 1.21 Satellite position related to the ground station.

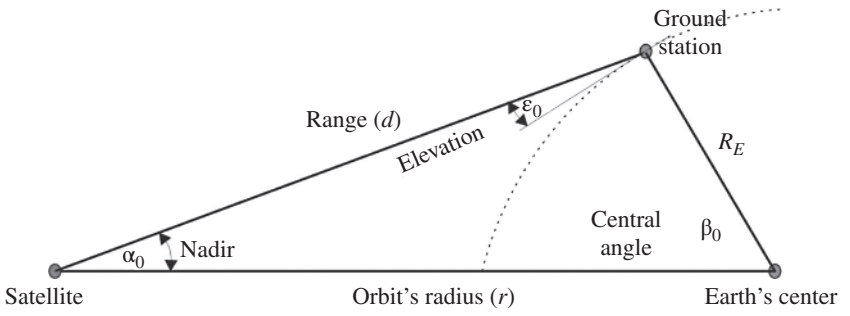

Figure 1.22 Ground station geometry.

Through this approach, the satellite to ground station range vector $\vec{d}$ is transformed to topo-centric-horizon system, which enables the look angles and the range from the ground station to the satellite to be calculated.

The triangle from the space view in Figure 1.21 is brought on plane, as a basic geometry between a satellite and ground station and depicted in Figure 1.22 (Gordon and Morgan 1993).

The two points indicate the satellite and ground station, and then the third is the Earth's center. Two sides of this triangle are usually known (the distance from the ground station to the Earth's center, $R_E = 6378\text{x}10^3$m and the distance from the satellite to Earth's center-orbital radius). The angle under which the satellite sees the ground station is called *nadir angle*. There are four variables

in this triangle: ε_0 is elevation angle, α_0 is nadir angle, β_0 is central angle, and d is slant range. As soon as two quantities are known, the other two can be found with the following equations:

$$\varepsilon_0 + \alpha_0 + \beta_0 = 90 \tag{1.51}$$

$$d\cos\,\varepsilon_0 = r\sin\,\beta_0 \tag{1.52}$$

$$d\sin\,\alpha_0 = R_E\,\sin\beta_0 \tag{1.53}$$

Sometimes one of the four parameters must be calculated in terms of any of the other three. The most needed parameter is the range d (distance from the ground station to the satellite). This parameter will be used during link budget calculation, and it is expressed through elevation angle ε_0. Applying cosines law for triangle at Figure 1.22. yields:

$$r^2 = R_E^2 + d^2 - 2R_E d\cos(90 + \varepsilon_0) \tag{1.54}$$

Solving Eq. (1.54) by d, yields:

$$d = R_E\left[\sqrt{\left(\frac{r}{R_E}\right)^2 - \cos^2\varepsilon_0} - \sin\varepsilon_0\right] \tag{1.55}$$

Substituting, $r = H + R_E$ at Eq. (1.55) we will get range as function of elevation angle ε_0 as:

$$d = R_E\left[\sqrt{\left(\frac{H + R_E}{R_E}\right)^2 - \cos^2\varepsilon_0} - \sin\varepsilon_0\right] \tag{1.56}$$

The range under the lowest elevation angle represents the worst link budget case, since that range represents the maximal possible distance between the ground station and the satellite.

Table 1.6 compares typical LEO, MEO, and GEO parameters (circular orbits) (Difonzo 2000). Data on this table are calculated under these considerations: systems have been seen under elevation angle $\varepsilon_o = 10°$, then Earth's radius $R_E = 6378$ km, Earth's surface area $A_{EARTH} = 511.2 \cdot 10^6$ km^2 and eccentricity $e = 0$.

Table 1.6 Comparison of parameters for LEO, MEO and GEO orbits.

Orbit	LEO	MEO	GEO
System	Iridium	ICO	INTELSAT
Inclination i (°)	86.4	45	0
Altitude H (km)	780	10 400	35 786
Semi major axis a (km)	7159	16 778	42 164
Orbit period (min)	100.5	360.5	1436.1
$(H + R_E)/R_E$	1.12	2.63	6.61
Earth central angle β_0 (°)	18.6	58.0	71.4
Nadir angle α_0 (°)	61.3	22	8.6
Slant range d (km)	2325	14 450	40 586
One-way time delay (ms)	2.6	51.8	139.1
Fraction of covered Earth's area	0.026	0.235	0.34

1.8 LEO MOST Satellite and Ground Stations

In 1997, anticipating new microsatellite altitude control technology, a team of scientists proposed a project to the Canadian Space Agency (CSA) to obtain astronomical photometry of unprecedented precision from a microsatellite. The following year, this project was approved and defined as: Microvariability and Oscillations of Stars (MOST). The MOST astronomy mission under the CSA Small Payloads Programs is the first Canada's space science microsatellite and the first space telescope. The MOST science team used the satellite to conduct long-duration stellar photometry observations in space. These stellar ultra-precise photometry observations are accomplished using a 15 cm aperture optical telescope mounted in a small suitcase sized satellite bus (65 cm × 65 cm × 30 cm; 60 kg) as given in Figure 1.23 (MOST inside, 2019). The high photometric precise optical telescope was developed by the University of British Columbia, and the high-performance altitude control system was provided by Dynacon Enterprises Limited, Canada (Zee and Stibrany 2002). Simplified, the goals of the mission were to analyze the inner structure of stars, set a lower limit to the age of the universe and to search for Exoplanets.

The project MOST consists of a LEO MOST satellite and three ground stations in: Vancouver, Toronto, and Vienna. The satellite link operates on 2GHz band.

The MOST satellite carries instruments designed to observe stars within the satellites CVZ (continuous viewing zone) by measuring tiny light variations undetectable from Earth. MOST is designed to detect variations in the brightness of stars with high precision. This will allow the MOST science team to translate these variations of nearby stars into information about their internal structures and ages, through a technique known as a stellar seismology. In addition, MOST can be used to detect orbiting Exoplanets.[1] Figure 1.24 shows the MOST satellite concept. The MOST satellite is launched in the LEO.

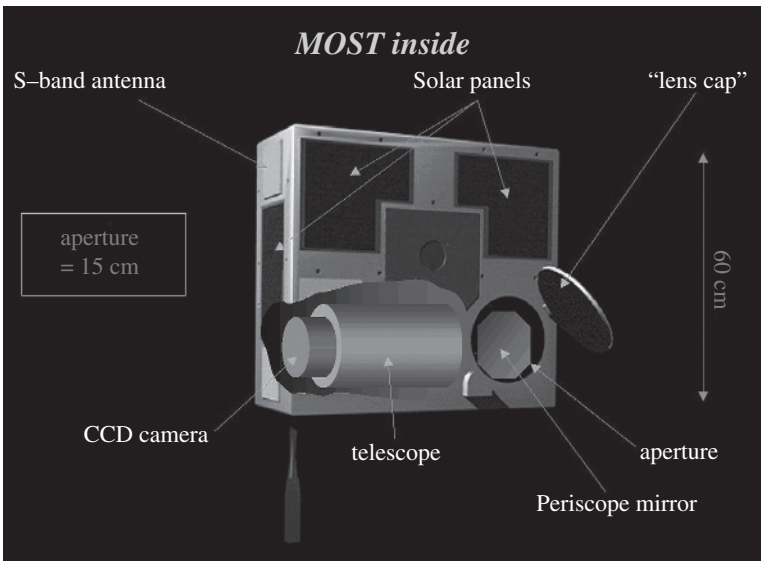

Figure 1.23 The MOST satellite inside.

1 An exoplanet is an extrasolar planet that orbits a star other than Earth's Sun.http://http://www.answers.com/topic/extrasolar-planet.

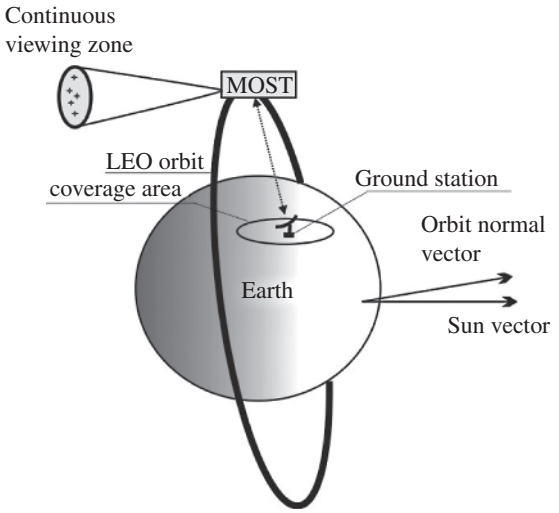

Figure 1.24 MOST satellite concept.

Table 1.7 MOST orbital elements.

Apogee	Perigee	Inclination	Orbital period
839.6 km	825.9 km	98.72 °	6085 s

The baseline orbit of the MOST is Sun-synchronous orbit; with 98° inclination at an altitude of around 820 km. Table 1.7 presents the main MOST orbital elements (Walker et al. 2003). MOST was successfully launched into its specified orbit on June 30, 2003, from the Khrunichev State Research and Production Space Centre in Plesetsk, Russia. MOST was injected into a low orbit with approximate altitude of 820 km. Contact with the satellite was established during it's the first pass over Toronto.

Inclination given in the Table 1.7 makes obvious Sun synchronization. The MOST satellite has a line-of-sight radio contact with each ground station 6–8 times per day when it is above the ground station. A pass over each ground station will last about 5–15 minutes (Carroll et al. 1998).

The project MOST consists of a LEO satellite and three ground stations, one of them in Vienna. The Vienna ground station system was set up at the Institute for Astronomy of the University of Vienna in cooperation with the Institute of Communications and Radio Frequency Engineering of the Vienna University of Technology, given in Figure 1.25 (Cakaj and Malaric 2007a).

In 2008, the MOST Satellite Project Team won the Canadian Aeronautics and Space Institute's Alouette Award, which recognizes outstanding contributions to advancement in Canadian space technology, applications, science, or engineering. The satellite MOST, by March 2019, having 66 487 revolutions was deactivated and closing its successful mission (MOST– A tiny satellite probes the mysteries of universe, 2019).

The author operated with the ground station in Vienna for a period of six months, so a lot of analyses and measurement given in this book stem from this project.

Figure 1.25 Vienna satellite ground station.

References

Botta, A. and Pescape, A. (2013). New generation satellite broadband internet service: should ADSL and 3G worry. TMA, co-located with IEEE INFOCOM 2013, Turin, Italy, April 2013.

Cakaj, S. (2021). The parameters comparison of the "Starlink" LEO satellites constellation for different orbital shells. *Frontiers in Communications and Networks.* 2: 643095. https://doi.org/10.3389/frcmn.2021.643095.

Cakaj, S. and Malaric, K. (2007a). Rigorous analysis on performance of LEO satellite ground station in urban environment. *International Journal of Satellite Communications and Networking* 25 (6): 619–643.

Cakaj, S. and Malaric, K. (2007b). *Isolation Measurement between Uplink and Downlink Antennas at Low Earth Orbiting Satellite Ground Station*, 24–26. Dubrovnik, Croatia: IEEE 19th International Conference on Applied Electromagnetics and Communications – ICECom.

Cakaj, S., Keim, W., and Malaric, K. (2007c). *Communications Duration with Low Earth Orbiting Satellites*, 85–88. Montreal: 4th IASTED International Conference on Antennas, Radar and Wave Propagation, IASTED, ARP.

Cakaj, S., Fischer, M., and Schotlz, L.A. (2009). *Sun Synchronization of Low Earth Orbits (LEO) through Inclination Angle*, 155–161. Austria: Innsbruck: Proceedings of the 28th IASTED International Conference on Modelling, Identification and Control, MIC.

Cakaj, S., Fitzmaurice, M., Reich, J., and Foster, E. (2010a). *Simulation of Local User Terminal Implementation for Low Earth Orbiting (LEO) Search and Rescue Satellites.* The Second International Conference on Advances in Satellite and Space Communications SPACOMM 2010, IARIA, 140–145. Athens, Greece: IEEE.

Cakaj, S., Kamo, B., Lala, A. et al. (2015a). The velocity increment for Hohmann coplanar transfer from different low earth orbits. *Frontiers in Aerospace Engineering* 4 (1): 35–41. https://doi.org/10.12783/fae.2015.0401.04.

Carroll, A.K., Zee, E.Z., and Matthews, J. (1998). The MOST Microsatellite mission: Canada's first space telescope. In: *12th Annual USU/AIAA Conference on Small Satellites*, Logan Utah, 1–19.

Cochetti, R. (2015). Low earth orbit (LEO) mobile satellite communications systems. In: *Mobile Satellite Communications Handbook*, 119–155. Hoboken, NJ: Wiley Telecom.

Constellation One Web, 2022, https://satellitemap.space/?constellation=oneweb.

De Selding, B.P. (2015). *Virgin, Qualcomm Invest in OneWeb Satellite Internet Venture*. Paris: SpaceNews.

Difonzo, F.D. (2000). *Satellite and Aerospace, the Electrical Engineering Handbook, Chapter 74*. Boca Raton: CRC Press LLC.

Elbert, B. (1999). *Introduction to Satellite Communication*. Norwood: Artech House Inc.

Foust, J. (2018) Data from Telesat to announce manufacturing plans for LEO constellation in coming months. SpaceNews. https://spacenews.com/telesat-to-announce-manufacturing-plans-for-leo-constellation-in-coming-months/ (Accessed January 17, 2021).

Garner, P., Cooke, D., and Haslehurst, A. (2009). *Development of a Scalable Payload Downlink Chain for Highly Agile Earth Observation Missions in Low Earth Orbit*, 529–534. Istanbul, Turkey: 4th International Conference Recent Advances in Space Technologies.

Golshan, N., Raferly, W., Ruggier, C., Wilhelm, M., Hagerty, B., Stockett, M., Cuccihissi, J., McWatters, D. (1996). *Low Earth orbiter demonstration terminal*, TDA Progress report 42–125, pp. 1–15, January – March 1996. http://ipnpr.jpl.nasa.gov/progress_report/42-125/125G.pdf (Sep. 2007).

Gordon, D.G. and Morgan, L.W. (1993). *Principles of Communication Satellites*. Sussex: Wiley.

Keim, W. and Scholtz, L.A. (2006). *Performance and Reliability Evaluation of the S-band, at Vienna Satellite Ground Station*, 5. Palma de Mallorca, Spain: Talk, IASTED, International Conference on Communication System and Networks.

Keim, W., Kudielka, V., and Scholtz, L.A. (2004). A scientific satellite ground station for an urban environment. In: *International Conference on Communication Systems and Networks, IASTED*, 280–284. Marbella, Spain.

List of spacecrafts deployed from the International Space Station, 2020. https://en.wikipedia.org/wiki/List_of_spacecraft_deployed_from_the_International_Space_Station

Losik, L. (1995). Final report for a low-cost autonomous, unmanned ground station operations concept and network design for EUVE and other NASA Earth orbiting satellites. *Technology Innovation Series*, Publication 666: Center for EUVE Astrophysics, University of California, Berkeley, California, July.

Maini, K.A. and Agrawal, V. (2011). *Satellite Technology*, 2e. West Sussex: Wiley.

Maral, G. and Bousquet, M. (2005). *Satellite communications systems*, 4e. West Sussex: Wiley.

MOST. (2019). A tiny satellite probes the mysteries of universe. https://www.asc-csa.gc.ca/eng/stellites/most/Default.asp.

MOST inside. (2019). MOST Inside (2019[SC1]). https://images.squarespace-cdn.com/content/v1/5115d365e4b0b8b2ffe27887/1399032938148-KJ7EDZKYNIN51DITJJQ9/ke17ZwdGBToddI8pDm48kJ3JQ3iwwc4BFbzDBp0TFgd7gQa3H78H3Y0txjaiv_0fDoOvxcdMmMKkDsyUqMSsMWxHk725yiiHCCLfrh8O1z5QHyNOqBUUEtDDsRWrJLTm9NV9qK7dJxdxXunNrepQQJ993frrKLqPB2KgwTjQ701ds2_F8iBDySdn6PX6ZVQV/image-asset.gif.

Nikolova, K.N. (2002). *Antenna Noise Temperature and System Signal-to-Noise Ratio*. Hamilton, Ontario, Canada: McMaster University.

Northern Lights Software Associates, (2003), www.nlsa.com.

Pultarova, T. and Henry, C. (2017) OneWeb weighing 2,000 more satellites. *SpaceNews* (Feb. 24). https://spacenews.com/oneweb-weighing-2000-more-satellites/.

Reisenfeld, S., Aboutanios, E., Willey, K., Eckert, M., Clout, R. and Thoms, A. (2007) The Design of the FedSat Ka Fast-Tracking Earth Sydney: Cooperative Research Center of Satellite Systems, Faculty of Engineering, University of Technology.

Richharia, M. (1999). *Satellite Communications Systems*. New York: McGraw Hill.

Roddy, D. (2006). *Satellite Communications*, 4e. New York: McGraw Hill.

Saunders, R.S. (1993). *Antennas and Propagation for Wireless Communication System*. Sussex: Wiley.

Sentinel-6 Michael Freilich, (2021), https://www.jpl.nasa.gov/missions/sentinel-6.

Sheetz, M. (2019). Data from Investing in Space: Amazon Wants to Launch Thousands of Satellites So It Can Offer Broadband Internet from Space. CNBC (April 4). https://www.cnbc.com/2019/04/04/amazon-project-kuiper-broadband-internet-small-satellite-network.html (Accessed January 17, 2021).

Sklar, B. (2005). *Digital Communication*, 2e. New Jersey: Prentice Hall PTR.

The real benefit of SpaceX-Starlink highspeed internet (2022) https://cerexio.com/blog/the-real-benefit-of-spacex-starlink-high-speed-internet

Van Allen radiation belt (2020) https://en.wikipedia.org/wiki/Van_Allen_radiation_belt.

Walker, G., Matthews, J., Kuschnig, R. et al. (2003). The MOST asteroseismology mission: Ultra, precise photometry from space. *Publication of the Astronomical Society of the Pacific, USA* 115 (811): 1023–1035.

Zee, E.R. and Stibrany, P. (2002). The MOST microsatellite: a low-cost enabling technology for future space science and technology missions. *Canadian Aeronautics and Space Journal* 48 (1), Canada: 43–51.